buildings

MDPI

Article

Development of Sustainable, Thermal-Insulated, and Load-Bearing Material and Modular Infill Wall Elements via 3D-Printed Formwork

Furkan Birdal [1,2,*] and Hasan Dilbas [1,2]

[1] Civil Engineering Department, Engineering-Architectural Faculty, Kırşehir Ahi Evran University, Kırşehir 40100, Türkiye; hasan.dilbas@ahievran.edu.tr
[2] FURKHASA R&D Engineering Technology Innovation and Consulting Inc., Erciyes Technopark, Kayseri 38039, Türkiye
* Correspondence: f.birdal@ahievran.edu.tr

Abstract

Unlike flammable organic insulation, non-combustible inorganic materials offer superior fire safety despite higher thermal conductivity. Recent research focuses on developing innovative, sustainable inorganic solutions using natural and waste-based raw materials. Accordingly, in this study, a thermal insulation material (TIM) design is presented for sustainable buildings. Specifically, white cement, fine and powdered pumice, hydraulic lime were formulated using Response Surface Methodology (RSM) with a Box–Behnken approach. A total of 46 mixtures were produced and cured under ambient conditions for 28 days before undergoing mechanical and physical testing in the experimental phase. ANOVA-validated quadratic models show all mixtures have low densities below 1.2 g/cm^3 and porosities of 35.52–39.62%. Optimal Run 23 achieves 11.55 MPa compressive strength, 2.53 MPa bending strength, and 0.25 W/m·K thermal conductivity. In addition, 3D-printed modular walls exhibit ductile behavior and maintain structural integrity up to 600 °C. Furthermore, a supplementary assessment of the optimal mixture modified with recycled concrete waste (Run-23+) demonstrated the viability of waste-aggregate integration for improved circular-economy performance. Microstructural analyses via XRD and SEM confirmed the dense formation of calcium silicate hydrate (C–S–H) networks and active pozzolanic reactions. Consequently, the present study demonstrates an advanced composite that combines low density with structural capacity, establishing a novel load-bearing thermal insulation material (LB-TIM). Moreover, by integrating this optimized LB-TIM mixture with custom designed 3D printed formwork technology, this study provides a novel and scalable manufacturing approach for sustainable, thermal-insulated and load-bearing material and modular infill wall elements.

Keywords: load-bearing thermal insulation material; Box–Behnken design; guarded hot-plate test; interlocking dry joint; pumice–lime–cement composite; 3D-printed formwork; sustainable modular infill wall; waste concrete upcycling

Check for updates

Academic Editors: Emilia Meglio, Giovanna Longobardi and George Wardeh

Received: 22 September 2026
Revised: 16 October 2026
Accepted: 22 October 2026
Published: 26 October 2026

Copyright: © 2026 by the authors. Licensee MDPI, Basel, Switzerland. This article is an open access article distributed under the terms and conditions of the Creative Commons Attribution (CC BY) license.

1. Introduction and Scope

1.1. Thermal Insulation and Environmental Imperatives in Buildings

The increasing need for comfortable indoor environments in the building sector drives a growing demand for effective thermal insulation materials. Buildings are significant consumers of energy, and utilizing suitable insulating materials is a crucial strategy to

enhance their energy performance and reduce energy consumption, even after many years of use. Consequently, improving the efficiency of thermal insulating materials (TIMs) that minimize heat transfer in buildings is a significant factor for energy saving and embodied carbon reduction. TIMs can broadly be categorized into two main types: inorganic and organic. Organic insulating materials, such as extruded polystyrene (XPS), expanded polystyrene (EPS), and polyurethane, are frequently used due to their low thermal conductivity. However, they are prone to burning and release toxic smoke when exposed to fire, which limits their widespread application in building construction. Inorganic insulating materials, including expanded perlite, pumice, lightweight expanded clay, vermiculite, and cementitious materials, are non-combustible and commonly used in the building sector, although their thermal conductivities are generally higher than those of organic materials [1].

1.2. Eco-Friendly Binders and the Challenge of Load-Bearing TIMs (LB-TIM)

There is a growing focus on developing materials that meet both technical and environmental requirements [1], leading to increased interest in sustainable, environmentally friendly, and traditional cementitious materials [1–5]. Research highlights the use of natural and waste-based materials like volcanic pumice powder, volcanic ash, and recycled concrete aggregates as supplementary cementitious materials or lightweight aggregates [1,6–8]. Lime-based insulating mortars have also been developed to enhance the thermal performance of building facades, sometimes incorporating lightweight aggregates such as expanded perlite [9,10]. Geopolymers, often derived from sources like metakaolin and fly ash, are explored for thermal insulation, utilizing various fillers and blowing agents to achieve desired properties [11]. Bio-based composites and materials recycled from industrial/mineral waste or packaging waste are also emerging trends [2–4]. The performance of thermal insulation materials is characterized by several key properties, including thermal conductivity, density, and porosity [1]. Low thermal conductivity is essential for minimizing heat transfer [1]. Low bulk density and high total porosity are often associated with good insulating properties [1,7]. Materials incorporating lightweight aggregates like pumice or expanded perlite tend to have lower densities and higher porosities compared to traditional materials [1,7,12]. Mechanical properties, particularly compressive strength, are also important for structural applications [1,6,11,13], although increasing the volume of lightweight fillers like expanded perlite often reduces compressive strength [1]. Developing an inorganic composite that simultaneously provides low thermal conductivity, low density, and high compressive strength, functioning as a Load-Bearing Thermal Insulation Material (LB-TIM) remains a significant engineering challenge. Durability aspects such as freeze–thaw resistance and chemical resistance are also considered in the development and evaluation of these materials [1,7]. It is well established that durability and thermal transport properties are intrinsically linked to the internal pore structure of materials; while higher porosity positively enhances thermal resistance, it can simultaneously introduce durability concerns. Thus, durability and heat transfer should be optimized for each TIM developed for its working conditions. Therefore, parameters must be selected meticulously based on specific environmental and operational conditions.

1.3. Fabrication: The Role of 3D-Printed Formworks in Modular Construction

Recent advancements include optimizing material compositions, exploring foaming techniques for materials like hydraulic lime [11,13], using volcanic particles in polymer composites [14], and incorporating supplementary cementitious materials like silica fume to enhance the strength of lightweight binders [1,3,7]. Studies also investigate the optimum insulation thickness for different materials and climate zones [2]. At the same time, digital

fabrication techniques, particularly 3D-printed formworks, are revolutionizing structural engineering by allowing the casting of geometrically complex, sustainable modular building wall elements. The integration of 3D-printed permanent or removable formworks with sustainable cementitious matrices eliminates traditional single-use formwork waste and ensures high dimensional tolerance for interlocking dry-joint mechanisms. Overall, combining advanced inorganic material formulations with digital fabrication strategies is critical for meeting the growing global demand for energy-efficient, sustainable, and scalable structural systems [1].

1.4. Research Objectives and Scope of the Study

In this study, a comprehensive experimental investigation was conducted to formulate and optimize an eco-friendly inorganic LB-TIM matrix. The constituent materials, including white cement, fine and powdered pumice, and hydraulic lime, were systematically proportioned using Response Surface Methodology (RSM) based on a Box–Behnken design. Additionally, recycled concrete aggregate was incorporated into the optimal formulation as a supplementary assessment to enhance ecological upcycling, reduce raw material consumption, and advance circular economy principles. Physical and mechanical characterization tests were carried out to evaluate the mixtures and identify the optimal formulation that meets standardized structural load-bearing requirements alongside low thermal conductivity. In conclusion, this study presents a comprehensive design framework for a Load-Bearing Thermal Insulation Material (LB-TIM) developed using Response Surface Methodology (RSM). The main theme of this research focuses on establishing a balanced composite matrix represented by the optimal pristine formulation while also evaluating the feasibility of circular-economy integration through recycled concrete waste incorporation. To explore practical structural applications, these optimized LB-TIM matrices were integrated with custom-designed 3D-printed PLA geometric formworks, offering an eco-friendly manufacturing approach for sustainable, thermally insulated, and load-bearing modular infill wall elements with an interlocking dry-joint assembly mechanism.

2. Materials and Methods

2.1. Materials

According to the report of "Notification on Expanding the Use of Green Cement with Low Carbon Emissions in Public Procurement Contracts" [15], clinker content reduction in cement production has been made an obligation. In addition, it has been suggested that the amount of clinker in cement production will gradually decrease over the years. This sustainable approach reduces embodied carbon emissions and lowers production costs. To decrease the carbon footprint of cement, CEM II, CEM III, and CEM IV were defined as green cement and proposed to encourage their widespread application, standing out for their environmental sustainability and technical performance [15]. For this reason, CEM II/A-LL 52.5 R white cement with reduced clinker content was used in the TIM mixtures. The research and application of this cement type in sustainable lightweight TIM mixtures are expected to contribute to modern green building standards. The physical and chemical properties of CEM II/A-LL 52.5 R are listed in Table 1. Hydraulic lime is a versatile binder used in construction, prized for its ability to set underwater and in moist conditions. Unlike non-hydraulic lime, it contains clay minerals that trigger a chemical reaction during curing, enhancing durability and strength. This makes hydraulic lime ideal for masonry infill walls, restoration work, and eco-conscious building applications. It allows breathability while resisting decay, contributing to long-lasting structures. Depending on its clay content, hydraulic lime is categorized into feebly, moderately, and eminently hydraulic types. Its

balance between flexibility and resilience makes it a sustainable alternative to cement in heritage conservation and modern green architecture.

On the other hand, milled pumice (MP) has been reported as a suitable mineral addition for cementitious building materials [16]. Due to its small particle size and amorphous silicate content, MP reacts with calcium- and sodium-bearing phases to form C-S-H, C-A-S-H, and N-A-S-H gel structures. Thus, MP was incorporated into the mix designs to exploit these pozzolanic characteristics. Sourced from Türkiye, the pumice utilized in this study served a dual purpose: MP as a mineral addition (<0.063 mm) and un-milled pumice (UMP) as a fine lightweight aggregate (<2 mm). Pumice aggregates (<2 mm) were used as natural aggregate replacements in specimen production. Lightweight aggregates typically feature a bulk density of less than 2.0 g/cm^3, and the incorporation of UMP significantly reduces the unit weight of the elements. Furthermore, the optimized particle packing and matrix densification achieved through this combination help transfer loads effectively. Thus, combining MP and UMP is critical not only to ensure that the TIM remains lightweight, but also to achieve high strength performance.

Concrete is ubiquitous in the construction industry, resulting in substantial waste generation from an annual global concrete production exceeding 10 billion tons [17]. Approximately 30–40% of this amount becomes concrete waste (CW) due to over-ordering, spillage, and demolition [18], yielding 3–4 billion tons of CW annually. To contextualize this volume, the annual global CW production is equivalent to a massive concrete block 3000 m high covering a 1 km^2 area. Addressing this issue sustainably is paramount, and utilizing CW as a recycled component in new cementitious materials represents an effective solution. In addition, concrete is widely recognized as the second most consumed material on Earth after water [19,20].

Consequently, various high-volume waste materials generated worldwide can be effectively integrated into sustainable construction applications. In this study, construction and demolition waste was processed and incorporated specifically into the supplementary evaluation of the optimal mixture (Figure 1) with the aim of creating a closed-loop recycling mechanism. This approach contributes to sustainable TIM manufacturing and reduces waste at the material lifecycle level instead of resorting to environmental disposal. Upcycling waste as functional construction components rather than treating it as refuse aligns directly with the sustainable development and economic targets of Türkiye, the European Union, and the United Nations. The recycled concrete aggregate used for the supplementary mixture (Run-23+) was obtained from waste materials generated after structural testing in a laboratory. To prepare the aggregate, the waste concrete was processed in a Los Angeles abrasion drum subjected to 500 revolutions. Following the mechanical crushing process, the material was sieved, and only the fraction passing through the 2 mm sieve was selected for mixture integration. Laboratory measurements indicated that this recycled aggregate possesses a bulk density of 2.2 g/cm^3 and a water absorption percentage of 7.8%.

To mitigate workability challenges in fresh mixtures resulting from the high water demand of fine binders and fine aggregate fractions, a polycarboxylate-based superplasticizer was incorporated into the mix design to achieve optimal flowability and casting behavior. Specifically, the superplasticizer dosage varies between 1.2% and 2.5% by weight of the binder to compensate for the varying water demand induced by the specific surface area and grading of the fine pumice fractions, thereby ensuring consistent workability and full experimental reproducibility.

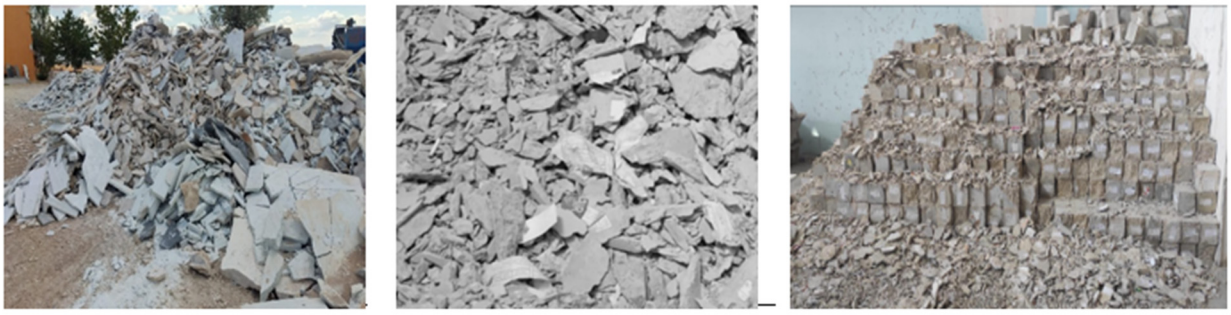


Figure 1. Waste concrete.

Table 1. The properties of CEM II/A-LL 52.5 R [21], Hydraulic Lime, and Pumice.

Binder	SiO_2 (%)	Al_2O_3 (%)	Fe_2O_3 (%)	CaO (%)	MgO (%)	SO_3 (%)	K_2O (%)	Na_2O (%)	LOI (%)	Blain (cm^2/g)	Density (g/cm^3)	Water Absorb.
CEM II/A-LL 52.5 R	20.1	3.63	0.25	64.80	1.36	3.52	0.25	0.25	5.50	4530	2.90	-
Hydraulic Lime (NHL 3.5)	12.9	0.7	0.2	66.8	0.7	0.8	0.12	0.04	17	11,000	0.6	-
Pumice	70	11.67	1.4	0.55	0.15	-	4.1	4.12	3.63	-	0.4–0.6	% 50

2.2. Methods and Experimental Design

In the first stage of the study, the Response Surface Methodology (RSM) was employed to evaluate the effects of individual variables and their synergistic interactions. RSM is widely utilized across various civil engineering applications to construct predictive mathematical models and optimize composite mix proportions. In this study, compressive strength test results served as the primary response variable within the RSM framework to optimize the constituent materials of the load-bearing thermal insulation material (LB-TIM). Among the traditional experimental designs for RSM, such as Central Composite Design (CCD) and Box–Behnken Design (BBD), the BBD approach was selected due to its higher efficiency in requiring fewer experimental runs. Design-Expert software Stat-Ease 360 version 25.0.8 64 bit [22] was used to generate the mixture design. Response Surface Methodology (RSM) combined with a Box–Behnken Design was implemented to optimize the process parameters and mix proportions. In this statistical framework, key independent variables were evaluated across designated low, center, and high levels (−1, 0, +1). A series of experimental runs generated by the Box–Behnken Design matrix was conducted to analyze both individual and interactive effects on the target responses. Quadratic regression models were subsequently fitted to the experimental data, and Analysis of Variance (ANOVA) was performed to validate the statistical significance, adequacy, and predictive capability of the established models. Consequently, a total of 46 experimental runs were designed, with the parameter ranges (expressed as a percentage by mass of the total matrix) summarized in Table 2. These proportion ranges were determined by taking into account preliminary trials in our laboratory work. The mixtures comprised white cement, water, milled pumice (MP), un-milled pumice (UMP), and hydraulic lime (Figure 2). In the second stage of the study, following the testing and mechanical evaluation of the 46 experimental runs, the optimal TIM mixture design was identified and further modified. Additionally, to eliminate any unit ambiguity and ensure 100% experimental reproducibility, the exact mix proportions by weight (g/3 specimens (40 × 40 × 160 mm)) for all 46 RSM experimental runs are comprehensively presented in Table 3. In this modified formulation, UMP was partially replaced with 50% concrete waste (CW) by volume to maximize ecological upcycling and advance circular economy principles.

Table 2. Ranges of RSM variables and unit definitions for mix optimization.

Component	Unit	Minimum Level (−1)	Maximum Level (+1)	Calculation Basis
White Cement	wt.%	4	25	Mass percentage of total matrix
Water	wt.%	20	50	Mass percentage of total matrix
Hydraulic Lime	wt.%	1	12	Mass percentage of total matrix
Un-milled Pumice	wt.%	25	50	Mass percentage of total matrix
Milled Pumice	wt.%	4	20	Mass percentage of total matrix

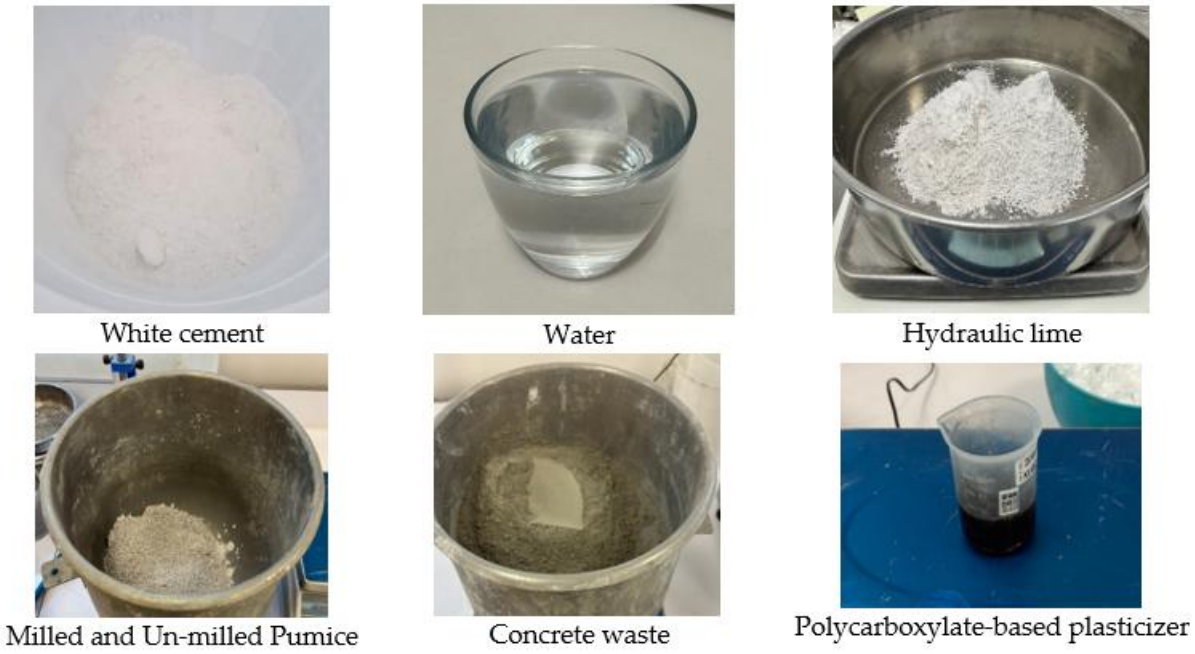


Figure 2. Components of TIM.

Table 3. Mix proportions by weight for the RSM design matrix (g/3 specimens (40 × 40 × 160 mm)).

No	Cement, g	Hydraulic Lime, g	Unmilled Pumice, g	Milled Pumice, g	Water, g
1	61	49	183	73	159
2	76	36	152	91	197
3	74	12	223	59	149
4	55	26	219	66	142
5	67	32	202	54	175
6	86	14	171	69	223
7	108	33	203	54	136
8	75	12	225	30	195
9	68	55	205	27	178
10	24	29	239	48	155
11	34	41	172	69	224
12	27	32	199	80	173
13	76	37	153	61	244
14	67	32	202	54	175
15	60	10	238	48	155
16	30	36	224	60	149

Table 3. *Cont.*

No	Cement, g	Hydraulic Lime, g	Unmilled Pumice, g	Milled Pumice, g	Water, g
17	67	11	200	53	213
18	55	26	220	44	176
19	98	29	183	73	158
20	67	32	202	54	175
21	61	29	182	73	194
22	123	37	154	62	200
23	99	49	186	49	161
24	30	12	221	59	192
25	76	36	227	30	151
26	109	33	204	27	177
27	67	32	201	80	134
28	67	32	202	54	175
29	77	62	155	62	201
30	67	32	202	54	175
31	87	42	174	69	174
32	60	29	242	24	157
33	60	29	241	48	120
34	68	32	203	27	217
35	87	42	175	35	227
36	61	49	184	49	197
37	68	54	204	54	136
38	27	54	203	54	176
39	107	11	201	54	174
40	67	32	202	54	175
41	30	36	225	30	195
42	27	32	201	53	214
43	88	27	221	44	144
44	55	44	222	44	144
45	66	11	199	79	172
46	98	29	184	49	196

2.3. Specimen Production, Curing, and Testing

TIM samples were produced under standard laboratory conditions (Figure 3). Following the mixing process, the fresh mixtures were cast into 40 × 40 × 160 mm molds. The filled molds were then consolidated on a vibration table until air bubbles ceased to emerge on the top surface. Since entrained air voids can form during fresh-state mixing, vibration applications are vital to ensure structural density. After 24 h, the samples were demolded and cured under standard laboratory conditions (24 ± 2 °C temperature and 50 ± 5% relative humidity (RH)) for 28 days. The cured 40 × 40 × 160 mm specimens were subjected to flexural and compressive strength tests in accordance with TS EN 196-1 regulations (Figure 3). The ultimate failure loads obtained from the bending and compression tests were used to calculate stress using Equations (1) and (2), respectively:

$$\sigma_c = \frac{F_c}{A} \tag{1}$$

$$\sigma_b = \frac{M}{I} y \tag{2}$$

where σ_c is the compressive strength in MPa, F_c is the maximum compression force in Newtons, A is the cross-sectional area where the force is applied in mm^2, σ_b is the bending strength in MPa, M is the maximum bending moment in N·mm, I is the moment of inertia in mm^4, and y is half the height of the beam specimen in mm.



Figure 3. Production and testing process of the samples.

2.4. Thermal Conductivity Characterization

To evaluate the thermal insulation performance of the developed LB-TIM specimens, thermal conductivity (λ-value) measurements were conducted at an accredited laboratory following the EN 12667 [23] standard using a guarded hot plate apparatus. Prismatic specimens with dimensions of 100 × 100 × 50 mm were conditioned at the lab until reaching constant mass to eliminate moisture interference prior to testing (Figure 4). Thermal conductivity measurements were recorded at a mean testing temperature range of 10 °C to 30 °C under steady-state heat flow conditions. The average value of identical samples was reported for each mix proportion to ensure reproducibility.

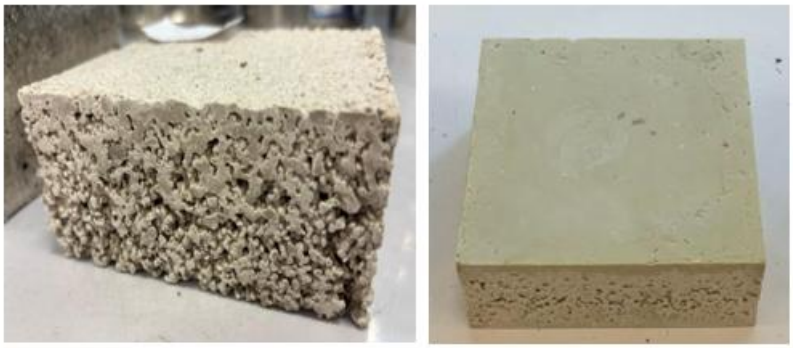


Figure 4. Test specimens of thermal conductivity characterization.

Although thermal insulation is a critical performance parameter, the Box–Behnken RSM optimization workflow focused primarily on mechanical strength (compressive and bending) and bulk density to ensure structural load-bearing capacity. Thermal conductivity measurements were intentionally designated as a validation metric for the final optimal formulation rather than a multi-objective optimization target, aiming to confirm the thermal performance of the structurally validated composite without extending the primary mechanical screening matrix.

2.5. 3D Printed Formwork

To scale up the optimized LB-TIM composite into functional building components, custom-designed interlocking modular forms were produced using digital fabrication technology. Polylactic acid (PLA) filaments were used to print precise, removable formworks on Fused Deposition Modeling 3D printers [24]. Furthermore, owing to the inherently low thermal conductivity of PLA compared to standard building matrices, continuous polymer elements do not act as high-conductivity thermal bridges [25]. Prior to casting the composite material, initial hollow PLA prototype unit elements were fabricated to

evaluate the geometric tolerance, interlocking fitability, and structural connectivity of the joint mechanisms (Figure 5). Following the verification of the joint behavior, the optimized LB-TIM mixture was poured directly into these 3D-printed PLA molds to form lightweight modular unit elements featuring rigid interlocking shear keys (Figure 5).

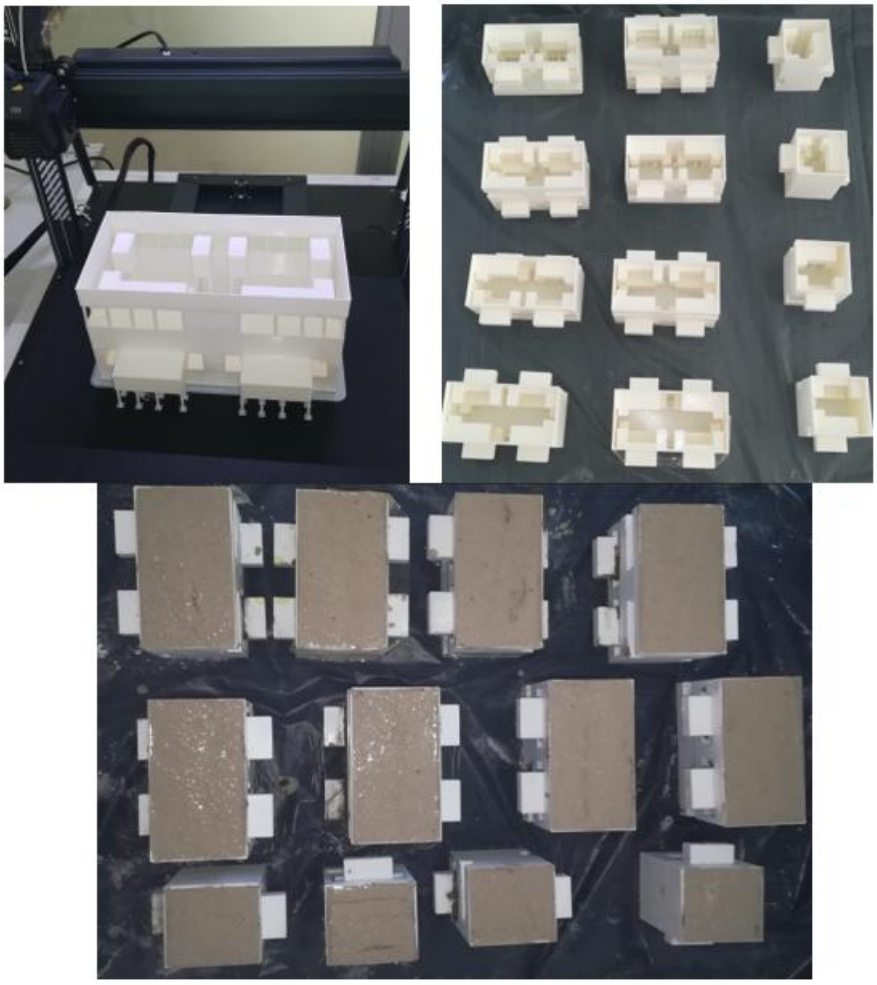


Figure 5. 3D-printed formwork of modular infill wall elements and LB-TIM casting.

2.6. Circular Economy Upcycling of Concrete Waste in the Optimized Mixture

To evaluate the feasibility of enhancing environmental sustainability without compromising the structural integrity of the optimized load-bearing thermal insulation material (LB-TIM), a supplementary trial was conducted based on the optimal mix. In this modified formulation (designated as Run. . .+), the fine lightweight aggregate fraction (un-milled pumice) was partially replaced with a 50% volume substitution of recycled concrete waste (CW). This targeted substitution strategy was implemented to investigate the upcycling potential of demolition by-products, thereby fostering circular economy principles within the manufacturing process. The preparation, mixing, casting, and curing procedures for the CW-modified mixture followed identical standardized protocols applied to the primary Box–Behnken design matrix, ensuring direct comparability in subsequent physical, mechanical, and thermal characterizations.

3. Results

3.1. First Stage of the Study: Mechanical Parameters of TIM Matrix

To determine the optimal mixture proportions for the Load-Bearing Thermal Insulation Material (LB-TIM), various constituent materials were incorporated into the mix designs.

The range and mixture proportions of component quantities are detailed in Tables 2 and 3, while the corresponding physical and mechanical test results are presented in Table 4. The primary objective of this initial evaluation was to assess the individual and synergistic effects of the TIM components on compressive strength, flexural strength, and density.

Table 4. Test results of TIM and standard deviations.

No	Bending Strength, MPa	Compressive Strength, MPa	Density, g/cm^3	Standard Deviation of Bending Strength	Standard Deviation of Compressive Strength	Standard Deviation of Density
1	1.71	7.06	0.97	0.038	1.30	0.029
2	1.59	7.46	1.05	0.100	1.23	0.060
3	1.96	5.39	0.75	0.065	1.15	0.027
4	1.43	5.12	0.75	0.136	1.25	0.062
5	1.6	5.38	0.92	0.131	1.27	0.048
6	1.93	4.15	0.86	0.136	0.59	0.057
7	1.6	4.6	0.79	0.100	1.33	0.015
8	2.13	3.67	0.91	0.297	0.83	0.072
9	1.59	4.61	0.86	0.075	1.27	0.074
10	0.98	2.14	0.80	0.038	0.62	0.062
11	0.88	4.02	0.89	0.038	0.72	0.066
12	1.21	5.48	0.97	0.065	0.59	0.084
13	0.92	4.09	0.95	0.000	0.57	0.080
14	N/A	N/A	N/A	N/A	N/A	N/A
15	0.51	1.16	0.57	0.000	0.36	0.008
16	0.84	2.78	0.69	0.065	0.62	0.059
17	1.61	3.54	0.85	0.100	0.47	0.057
18	1.59	1.8	0.74	0.065	0.71	0.056
19	2.45	10.93	0.96	0.065	1.92	0.023
20	N/A	N/A	N/A	N/A	N/A	N/A
21	0.79	4.23	0.98	0.075	0.68	0.062
22	2.09	11.19	1.08	0.038	1.26	0.028
23*	2.53	11.55	1.04	0.192	1.41	0.023
24	0.84	1.88	0.69	0.000	1.31	0.081
25	2.14	3.33	0.73	0.075	0.48	0.035
26	1.99	8.3	0.93	0.038	2.14	0.022
27	1.83	4.81	0.80	0.113	0.97	0.013
28	N/A	N/A	N/A	N/A	N/A	N/A
29	1.59	5.39	1.05	0.100	2.07	0.051
30	N/A	N/A	N/A	N/A	N/A	N/A
31	2.63	5.14	1.04	0.136	0.58	0.023
32	0.88	1.67	0.67	0.065	0.63	0.060
33	0.73	2.43	0.67	0.038	0.34	0.026
34	1.39	2.87	0.85	0.113	0.62	0.043
35	1.57	3.2	0.93	0.113	0.71	0.087
36	1.46	4.48	0.93	0.136	0.61	0.045
37	1.64	3.8	0.71	0.065	0.77	0.025
38	0.36	2.25	0.82	0.000	0.66	0.069
39	2.71	4.76	0.94	0.100	1.17	0.063
40	N/A	N/A	N/A	N/A	N/A	N/A
41	0.8	2.81	0.85	0.075	0.91	0.071
42	0.45	2.94	0.86	0.038	0.65	0.070
43	N/A	N/A	N/A	N/A	N/A	N/A
44	1.35	3.36	0.79	0.075	0.72	0.036
45	1.46	5.62	0.93	0.100	0.96	0.034
46	1.99	5.68	0.98	0.131	0.92	0.067

N/A: Data not available due to severe segregation or loss of structural integrity during demolding.
23*: Run 23.

Among the 46 experimental runs formulated in the Box–Behnken design matrix, six mixtures (Runs 14, 20, 28, 30, 40, and 43) resulted in N/A values due to structural collapse during demolding. The primary physical mechanism behind these failures was the excessive dryness of the fresh mixtures, caused by an insufficient water-to-binder ratio relative to the high-water absorption capacity of the porous pumice aggregate fractions. This extreme dryness severely restricted matrix compaction and fresh-state cohesion, preventing proper structural formation. To prevent skewing the response surface regression and violating ANOVA normality assumptions, these six untestable mixtures were excluded from the mathematical RSM model. The remaining 40 successful experimental runs ensured robust design space coverage, yielding high model fitting accuracy (R^2: 0.6641–0.7595, Adjusted R^2: 0.6147–0.7241) and reliable predictive performance across the viable mix space (Table 5).

Table 5. Summary of quadratic model ANOVA and fit statistics for compressive strength, bending strength, and density [22].

Response Variable	Sum of Squares	df	Mean Square	F-Value	*p*-Value	Fit Statistics (R^2, Adj-R^2, Predict R^2)
Compressive Strength (MPa)	158.1	5	31.62	13.45	<0.0001	R^2: 0.6641 Adj R^2: 0.6147 Predict R^2: 0.5378 Adeq. Precision: 12.77
Bending Strength (MPa)	10.10	5	2.02	16.30	<0.0001	R^2: 0.7056 Adj R^2: 0.6623 Predict R^2: 0.6042 Adeq. Precision: 13.56
Density (g/cm^3)	0.4556	5	0.091	21.47	<0.0001	R^2: 0.7595 Adj R^2: 0.7241 Predict R^2: 0.6459 Adeq. Precision: 18.97

Evaluation of the 46 experimental runs in the RSM design matrix revealed that Run 23 exhibited superior overall mechanical performance, achieving the maximum compressive strength of 11.55 MPa and a flexural strength of 2.53 MPa at a bulk density of 1.04 g/cm^3. This significant enhancement in mechanical capacity is primarily attributed to the optimized balance between the binding matrix (white cement and hydraulic lime) and the aggregate packing density, which minimized macro-porosity while preserving structural integrity. Consequently, owing to its ability to meet structural load-bearing demands while maintaining a low unit weight, the formulation of Run 23 was selected as the optimal baseline matrix for the second stage of the study. To comprehensively validate the adequacy and predictive reliability of the quadratic response surface models, residual diagnostics and optimization equations were thoroughly evaluated. As illustrated in Figure 6, the diagnostic plots, including the normal plot of residuals, residuals versus predicted values, predicted versus actual values, and Cook's distance, demonstrate that the residuals are normally distributed, randomly scattered within acceptable limits, and free of severe outliers, thereby confirming the statistical assumptions of the ANOVA.

Furthermore, the mathematical relationships derived from the analysis enable accurate prediction of the mechanical properties and density within the studied experimental domain. The final quadratic regression equations in terms of coded factors are expressed as follows [22]:

$$\text{Compressive Strength } (Y_1): 16.76A + 11.46B - 9.37C + 13.98D - 9.16E + 41.64CE \quad (3)$$

$$\text{Bending Strength } (Y_2)\text{: } 5.67A + 1.49B - 1.32C + 2.16D - 2.02E + 11.26CE \quad (4)$$

$$\text{Density } (Y_3)\text{: } 1.22A + 1.32B + 0.0249C + 1.22D + 0.5967E + 2.05CE \quad (5)$$

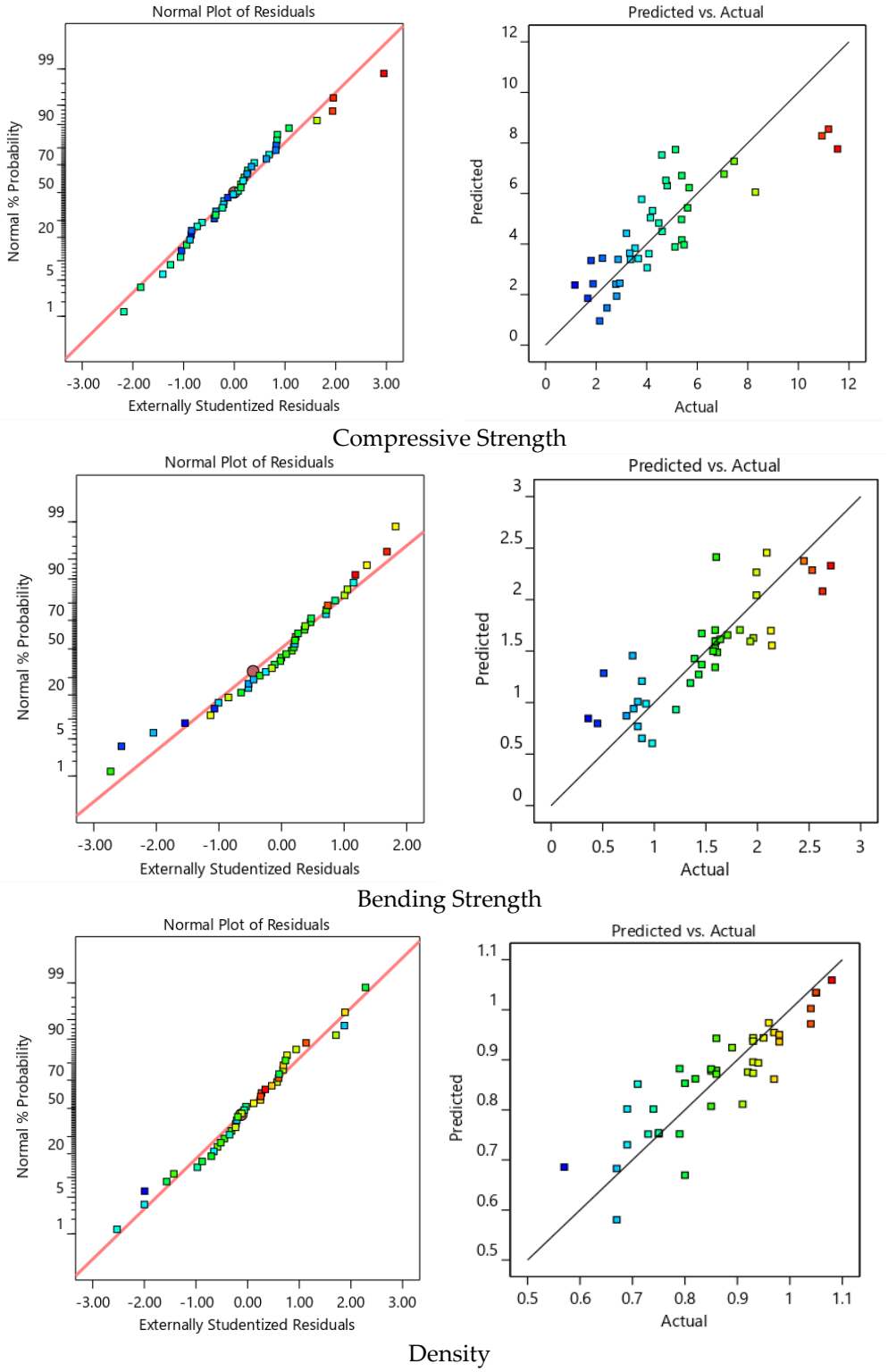


Figure 6. Diagnostic plots for the developed models [22].

In this study, the mechanical and physical properties of the composite materials were modeled using variables. The parameters are defined as follows: A represents cement, B denotes hydraulic lime, C corresponds to un-milled pumice, D indicates milled pumice, and E stands for water. The interaction term CE reflects the combined effect of un-milled

pumice and water. These validated models ensure reliable optimization of the composite mixtures within the designated design space.

3.2. Thermal Conductivity Evaluation of LB-TIM Run 23 Mixture

In addition to mechanical characterization, thermal conductivity (λ-value) measurements were performed on selected representative matrix formulations using the guarded hot plate apparatus according to EN 12667 [23]. The thermal conductivity value of the optimized LB-TIM Run 23 mixture was determined as 0.25 W/mK. The achieved thermal conductivity confirms that the optimized composite successfully bridges the gap between traditional load-bearing capacity and high-performance thermal insulation, fulfilling the functional requirements for structural LB-TIM building envelopes. In this study, primary optimization efforts initially focused on achieving superior mechanical and physical properties. Once Run 23 was identified as the optimal formulation exhibiting the highest mechanical performance, thermal conductivity testing was conducted specifically on this mixture. Given the exceptionally favorable thermal results obtained, significantly outperforming conventional industry products, further thermal testing across all secondary mixes was deemed unnecessary, as Run 23 fully demonstrated the material's viability as an effective structural thermal insulation composite.

3.3. Structural Load-Bearing Qualification of Optimized TIM Matrix (Run 23)

Among the 46 experimental runs evaluated in the RSM design matrix, Run 23 exhibited the superior overall mechanical performance, achieving a maximum compressive strength of 11.55 MPa and a bending strength of 2.53 MPa at a bulk density of 1.04 g/cm^3. These specific metrics were prioritized to optimize structural load-bearing capacity while satisfying target density criteria, identifying Run 23 as the most balanced formulation for comprehensive qualification. The recorded compressive strength of 11.55 MPa significantly exceeds the standardized minimum thresholds specified by EN 771-3 [26] for structural load-bearing masonry units (2.5–5.0 MPa), while fully satisfying the structural safety requirements of TS EN 772-1 [27] and the Türkiye Building Earthquake Code (TBEC) [28], which prescribes a minimum unit compressive strength of 5.0 MPa for load-bearing masonry walls in seismic zones. Unlike conventional lightweight cementitious composites in the literature that trade structural integrity for reduced density, the matrix formulation of Run 23 successfully bridges high mechanical capacity with lightweight characteristics, confirming its qualification as a structural-grade Load-Bearing Thermal Insulation Material (LB-TIM) matrix for the 3D-printed modular wall assembly. Lightweightness is a core parameter that acts as a vital bridge between thermal efficiency and structural integrity. While high mechanical strength ensures load-bearing capacity, maintaining a low density is equally essential to achieve the desired thermal insulation performance without imposing excessive dead loads.

3.4. Load-Bearing Sustainable Modular Infill Wall Elements and Modular Wall Assembly

To demonstrate the practical application and structural scalability of the optimized material, unit modular elements and their corresponding wall assemblies were fabricated using the developed LB-TIM composite. The manufacturing process utilized 3D-printing technology to produce high-precision PLA formworks. The fresh LB-TIM slurry was directly cast into these customized geometric formworks to produce sustainable modular infill wall units. Upon curing, the modular units' precise interlocking alignment ensures seamless dry joint wall assembly without requiring traditional mortar bedding layers. The successfully constructed prototype wall suggests that casting the optimized LB-TIM matrix into 3D-printed modular formworks presents a promising, lightweight, and sustainable approach for mortarless load-bearing infill wall construction (Figure 7). Figure 7 illustrates

the 1/2-scaled unit element with dimensions of 75 × 125 × 62.5 mm, corresponding to the full-scale unit element of 150 × 250 × 125 mm, as well as the modular wall with dimensions of 500 × 500 mm constructed from these scaled unit elements.



Figure 7. Load-Bearing Sustainable Modular Wall Elements and Modular Infill Wall Prototype.

3.5. Evaluation of Diagonal Tension and Shear Behavior of Modular Assemblies

To quantitatively evaluate the structural performance and failure mechanisms of the interlocking 500 × 500 mm dimensions modular wall system, diagonal tension tests were conducted on assembled specimens (Figure 8). Unlike brittle failure modes typically observed in traditional masonry or unreinforced mineral matrices, the quantitative load–displacement curves obtained from these tests demonstrated a controlled, ductile-failure response. The presence of the composite core–shell configuration, combined with the structural continuity provided by the interlocking joints, enabled significant energy dissipation and post-peak deformation capacity, substantiating the stable structural integrity of the modular assemblies under shear stress (Figure 9).

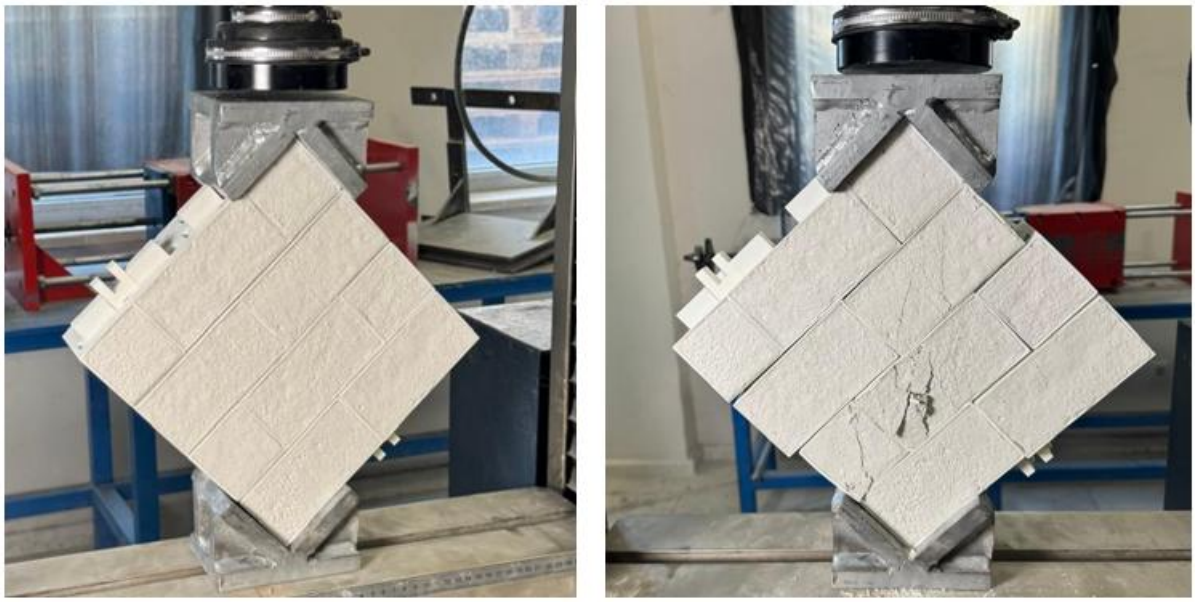


Figure 8. Experimental setup and configuration of the diagonal tension test on modular wall assemblies.

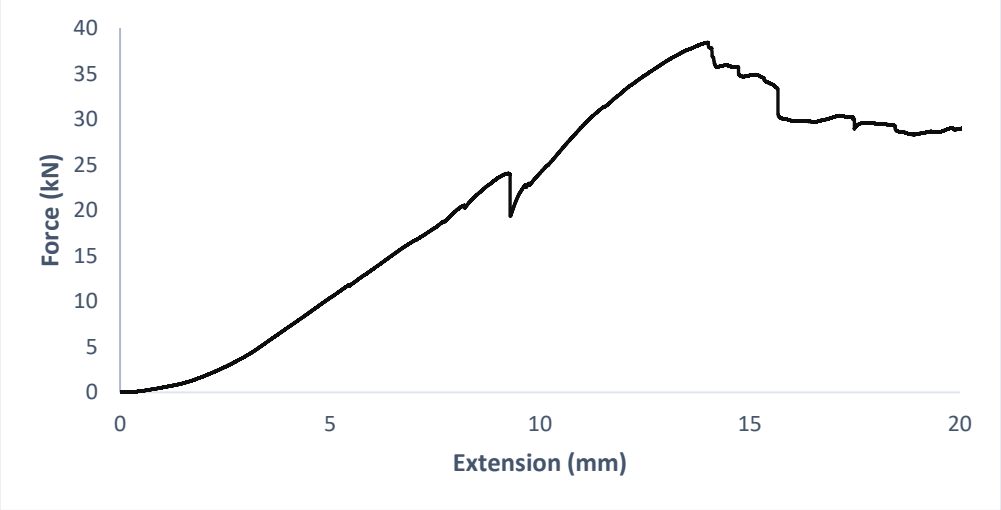


Figure 9. Load–displacement curve obtained from the diagonal tension test of the modular wall assembly.

3.6. Sustainability Focus

The developed modular infill wall system provides significant environmental advantages that align with sustainable construction paradigms. First, the core matrix utilizes an optimized, lightweight thermal insulation composite (LB-TIM) with low bulk density (1.04 g/cm^3), which substantially reduces raw material consumption, dead loads, and resource depletion compared to traditional heavy concrete units. Second, the integration of 3D-printed PLA formwork offers an eco-friendly manufacturing pathway by enabling precise, digital fabrication and eliminating single-use wooden or metallic formwork structures. Furthermore, the interlocking dry-joint mechanism eliminates the need for cement-based mortar bedding layers during wall assembly, thereby minimizing site-level environmental impacts associated with field mortar preparation and transport. The seamless recyclability potential of the PLA framework combined with the high operational thermal efficiency (λ = 0.25 W/mK) further lowers operational energy consumption over the building lifecycle, offering the proposed system as a viable sustainable structural wall alternative.

3.7. Performance Evaluation of the Recycled Concrete Waste Incorporated Mixture (Run-23+)

To evaluate the practical implications of incorporating recycled concrete waste (CW) into the optimized matrix, the physical, mechanical, and thermal properties of the Run-23+ mixture were compared against the pristine optimal mix (Run-23). The incorporation of 50% CW volume substitution resulted in a compressive strength of 8.81 MPa, successfully satisfying structural load-bearing requirements despite a moderate reduction compared to the pristine mix. While the bulk density increased to 1.46 g/cm^3 and the thermal conductivity adjusted to 0.39 W/mK due to the denser nature of the recycled aggregate, the material retains sufficient structural capacity. These findings confirm that upcycling concrete demolition waste into the LB-TIM framework offers a viable trade-off between circular economy targets and structural performance, validating the proposed upcycling approach for sustainable building applications.

3.8. High-Temperature Behavior and Thermal-Safety Performance of the LB-TIM Composite System

To evaluate the thermal safety and high-temperature structural performance of the proposed modular wall system, a multi-stage experimental investigation was conducted. First, preliminary oven-exposure tests on standalone 3D-printed PLA formworks at 100 °C

and 180 °C demonstrated that while empty polymer formworks undergo severe thermal softening and dimensional distortion, their integration within the composite assembly behaves differently (Figure 10).

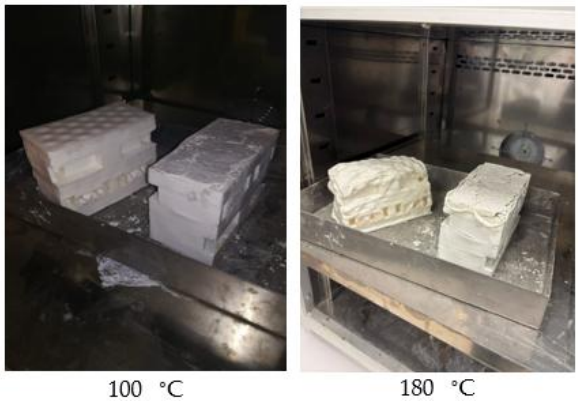


Figure 10. Thermal behavior and structural form during oven exposure testing.

Furthermore, to assess the fire-safety and thermal limits of the mineral-based core, LB-TIM matrix cubes were subjected to elevated thermal exposure in a muffle furnace (Figure 11) at 400 °C, 600 °C, and 800 °C. The residual compressive strength results, summarized in Table 6, indicate that the material retains substantial structural integrity under moderate-to-high thermal stress, maintaining 7.72 MPa and 8.84 MPa even after exposure to 400 °C and 600 °C, respectively, before reaching its structural boundary at 800 °C. These findings suggest that the core–shell synergy can enable the heavy mineral matrix to act as an effective thermal shield, potentially restraining the inner boundaries of the formwork and preserving overall load-bearing geometry even if the exterior PLA skin softens.



Figure 11. The muffle furnace during elevated temperature exposure tests.

Table 6. Residual compressive strength of the LB-TIM matrix after high-temperature exposure.

Specimen Name	Exposure Temperature (°C)	Compressive Strength (MPa)
Reference	20	11.55
400 °C	400	8.84
600 °C	600	7.72
800 °C	800	No result obtained (Structural integrity lost)

3.9. Water Absorption and Porosity Characteristics

To evaluate the basic durability and transport properties governing the service-life reliability of the developed insulation material, water absorption and permeable porosity tests were conducted in accordance with ASTM C642 [29]. As detailed in Table 7.

Table 7. Summary of water absorption capacity, density, and permeable pore volume characteristics of the insulation composite specimens evaluated in accordance with ASTM C642 [29].

Test Specimen	Absorption Capacity (%)		Densities (g/cm^3)				Permeable Pore Volume (%)
	After Immersion	After Immersion and Boiling	Dry Bulk Density	Saturated Bulk Density (Immersion)	Saturated Bulk Density (Boiling)	Apparent Density	
1	33.52	33.93	1.08	1.45	1.45	1.71	36.73
2	34.36	35.06	1.13	1.52	1.53	1.87	39.62
3	34.43	34.86	1.12	1.50	1.51	1.83	39.00
4	33.29	34.52	1.11	1.49	1.50	1.81	38.47
5	34.50	34.90	1.02	1.37	1.37	1.58	35.52
6	34.38	34.79	1.05	1.41	1.41	1.65	36.49
7	34.69	34.97	1.09	1.47	1.47	1.76	38.13
8	33.59	33.85	1.11	1.49	1.49	1.78	37.66
9	34.23	34.86	1.03	1.38	1.38	1.60	35.76

The ASTM C642 test results indicate that the dry bulk densities of the insulation specimens range from 1.02 g/cm^3 to 1.13 g/cm^3, while the apparent densities vary between 1.58 g/cm^3 and 1.87 g/cm^3. Furthermore, the water absorption capacities recorded after immersion and after immersion-and-boiling are between 33.29–34.69% and 33.85–35.06%, respectively, with permeable pore volumes ranging from 35.52% to 39.62%.

3.10. Microstructural Characterization

To understand the micro-level mechanisms behind the mechanical and thermal performance, representative microstructural analyses via X-ray diffraction (XRD) (Figure 12) and scanning electron microscopy (SEM) (Figure 13) were conducted on sample Run 23.

As evidenced by the XRD pattern, the binder matrix exhibits sharp characteristic peaks corresponding to calcite (∼29.4°), portlandite (∼18°), and quartz phases, alongside a broad amorphous hump associated with the reactive components of the fine pumice fractions. The SEM micrographs further display dense networks of fibrous and needle-like calcium silicate hydrate (C–S–H) crystals, confirming active pozzolanic reactions between the fine pumice and the binder paste. These microstructural features, combined with the porosity and density data, demonstrate how matrix densification improves mechanical strength, while micro-pores contribute to thermal insulation.

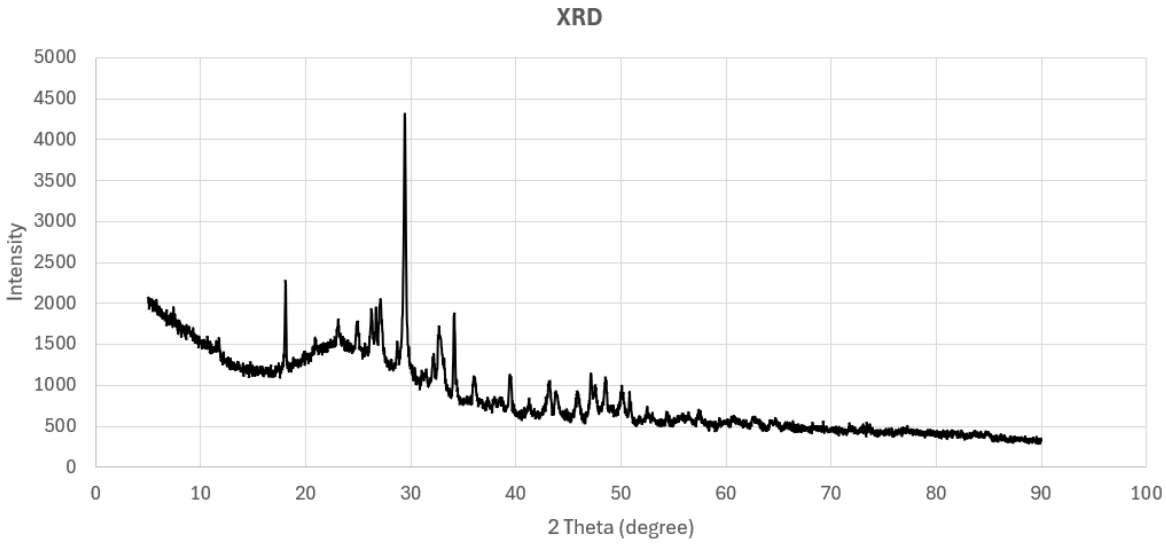


Figure 12. XRD pattern of the representative specimen (Run 23).

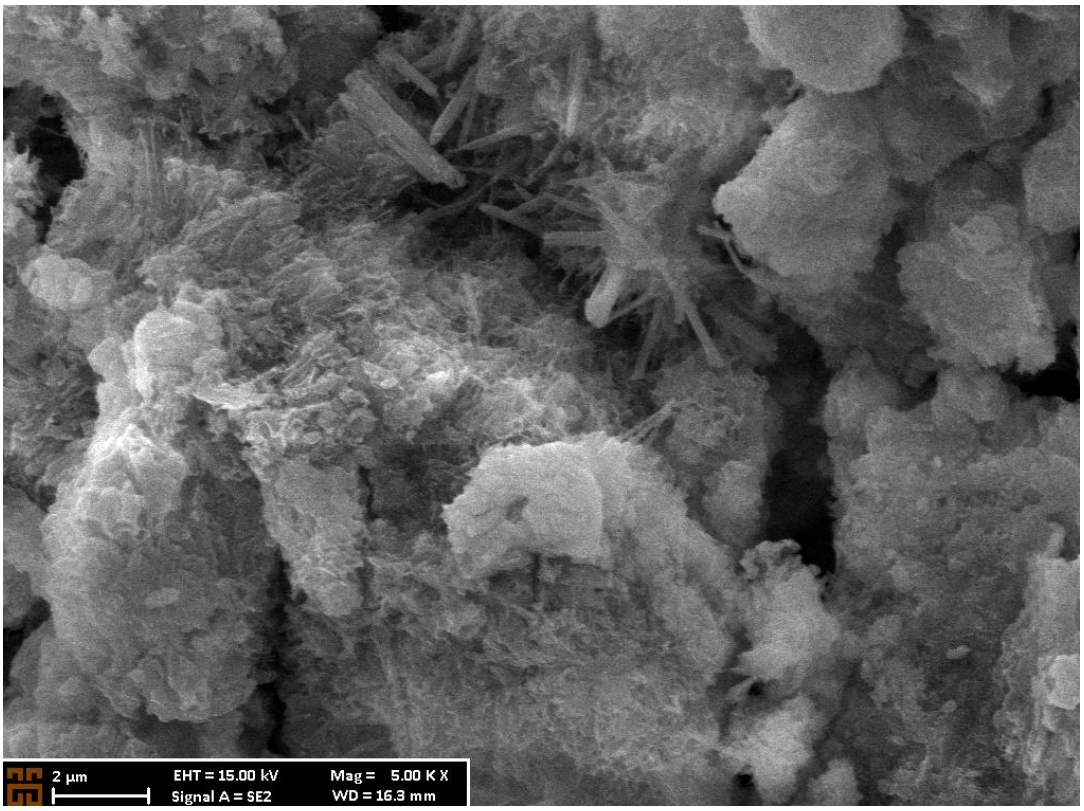


Figure 13. SEM micrograph of the representative specimen (Run 23).

4. Discussions

The development of multifunctional load-bearing thermal insulation materials (LB-TIMs) that combine structural performance, operational thermal efficiency, and environmental sustainability has become a central focus in contemporary construction research. In this study, a novel composite material was formulated using CEM II white cement, hydraulic lime, milled and un-milled pumice, with an additional evaluation incorporating recycled concrete waste. The experimental design employed the Box–Behnken Design within the framework of Response Surface Methodology (RSM), allowing for a systematic evaluation of the main effects and synergistic interactions among key mix parameters. The

optimal mix design (Run 23) achieved a compressive strength of 11.55 MPa with a bulk density of 1.04 g/cm^3, which places it within the class of structural-grade lightweight composites suitable for load-bearing infill wall applications. This mechanical capacity significantly exceeds the minimum 5.0 MPa threshold prescribed by TS EN 772-1 and the Türkiye Building Earthquake Code (TBEC) for structural load-bearing masonry units. However, this compliance specifically addresses the LB-TIMs developed within the scope of this study. For modular unit assemblies, scaled diagonal shear tests detailed in Section 3.5 were conducted. In these tests, the ductility and joint performance were evaluated at the wall scale rather than on an individual unit basis. These results are consistent with previous studies exploring lightweight mortars incorporating recycled aggregates and pozzolanic materials [30,31]. Thermal conductivity measurements yielded an optimal value of 0.25 W/(m·K), positioning the material within the highly effective thermal insulation range. This performance is comparable to pumice-based mortars studied by Akpınar and Koçyiğit [32], yet the present mix offers superior mechanical integrity due to the hybrid binder system. The inclusion of hydraulic lime contributed to long-term strength development through pozzolanic reactions, as previously reported by Velosa and Cachim [33]. Furthermore, the utilization of recycled concrete waste (Run 23+) directly supports circular economy principles and aligns with sustainability frameworks in Europe reported by Colangelo et al. [34]. A key observation in this study was the trade-off between workability and strength, particularly influenced by the proportion of ultra-fine pumice and water content. This trade-off arises because the high specific surface area of ultra-fine pumice significantly increases water demand, which can reduce flowability if not properly balanced. Conversely, while excess water improves workability, it compromises matrix densification and compressive strength. Thus, optimizing the water-to-binder ratio was essential to balance adequate workability during mixing with high structural integrity after curing. Beyond material-level performance, the practical integration of the optimized LB-TIM matrix into 3D-printed PLA formworks validates its application at the component and assembly levels. The outer PLA shell provided effective lateral confinement during compression, converting the typical brittle splitting of conventional masonry into a controlled, ductile failure mechanism characterized by progressive micro-cracking (Figure 14).



Figure 14. Pre-Test Evaluation of Unit Element Compressive Behavior.

Furthermore, the developed modular system offers significant sustainable advantages. The proposed LB-TIM system presents a viable, lightweight, and sustainable structural wall alternative for modern construction [35].

5. Conclusions

This study successfully formulated and evaluated a novel structural-grade load-bearing thermal insulation material (LB-TIM) utilizing Box–Behnken Design. The key findings are summarized as follows:

- Material Performance: The optimal formulation (Run 23) achieved an ideal balance of mechanical strength and thermal insulation, comfortably surpassing standard structural thresholds set by TS EN 772-1 and TBEC [28]. The hybrid binder system, combining white cement and hydraulic lime, ensured robust long-term stability through pozzolanic reactions.
- Circular Economy Integration: The incorporation of recycled concrete waste (Run-23+) validated the feasibility of upcycling construction waste without compromising structural viability, aligning with circular economy objectives.
- Component-Level Innovation: Integrating the LB-TIM matrix with 3D-printed PLA formwork and an interlocking dry-joint system established a viable, mortarless modular wall solution. The PLA casing effectively enhanced structural ductility, promoting progressive micro-cracking over brittle failure.

Overall, the synergy between optimized pozzolanic binders, recycled aggregates, and digital fabrication provides a promising pathway for sustainable, high-performance modular masonry systems.

6. Limitations and Future Recommendations

This study focused primarily on material-level characterization and short-term mechanical and thermal evaluations of unit modular elements under laboratory conditions, while long-term strength evolution (e.g., at 90 and 180 days to account for the delayed pozzolanic reactions of hydraulic lime), thermal conductivity evaluations across wider service temperature ranges (including sub-zero and elevated thermal conditions), and long-term durability and real-world environmental exposure were not assessed. Long-term durability, fire resistance, hygrothermal behavior, and real-world environmental exposure were not assessed. Furthermore, while full-scale unit modular elements and preliminary prototype wall assemblies were successfully demonstrated, comprehensive structural testing such as full-scale wall compression, shear capacity, out-of-plane bending, and dynamic cyclic/seismic performance of the dry-joint interlocking system remains beyond the scope of this work. Additionally, the industrial scalability, automated manufacturing feasibility of 3D-printed formworks, and overall cost-effectiveness of the proposed LB-TIM system require further investigation before practical implementation in large-scale construction projects.

Despite these boundaries, this research contributes to the growing body of literature on sustainable construction materials by offering a validated mix design and modular framework that balances structural strength and thermal insulation. Future studies should prioritize evaluating the long-term strength evolution of hydraulic-lime-containing mixtures over extended curing periods (90 and 180 days) alongside full-scale structural testing on assembled modular wall segments, including shear wall evaluations and joint interface dynamics under combined axial and lateral loading. Moreover, the material-level performance of the LB-TIM matrix could be further enhanced by incorporating internal curing strategies to mitigate autogenous shrinkage and by integrating discrete fibers (e.g., natural or recycled synthetic fibers) to improve tensile capacity, crack-bridging performance, and flexural toughness [36,37]. Investigating thermal conductivity behavior under sub-zero and elevated service temperatures, long-term durability under harsh climatic conditions, freeze–thaw cycles, fire performance, and thermal bridging effects across dry joints will also be critical to assess real-world field applicability. Finally, conducting a comprehensive

Life Cycle Assessment (LCA) alongside cost–benefit and supply-chain analyses will further support the seamless integration of 3D-printed LB-TIM modular systems into mainstream sustainable construction practices.

Author Contributions: F.B.: Methodology, data curation, conceptualization, writing paper, review paper, supervisor. H.D.: Investigation, data curation, methodology, writing paper, review paper. All authors have read and agreed to the published version of the manuscript.

Funding: This research received no external funding. This research was carried out with the funding provided under project number 2240086 within the scope of the TÜBİTAK 1812 program conducted by FURKHASA Inc.

Data Availability Statement: The raw data supporting the conclusions of this article will be made available by the authors on request.

Conflicts of Interest: Authors Furkan Birdal and Hasan Dilbas were employed by the company FURKHASA R&D Engineering Technology Innovation and Consulting Inc., Erciyes Technopark. All authors declare that the research was conducted in the absence of any commercial or financial relationships that could be construed as a potential conflict of interest.

References

1. Rashad, A.M.; Essa, G.M.F.; Morsi, W.M. Traditional Cementitious Materials for Thermal Insulation. *Arab. J. Sci. Eng.* **2022**, *47*, 12931–12943. [CrossRef]
2. Ali, A.; Issa, A.; Elshaer, A. A Comprehensive Review and Recent Trends in Thermal Insulation Materials for Energy Conservation in Buildings. *Sustainability* **2024**, *16*, 8782. [CrossRef]
3. Pawłosik, D.; Cebrat, K.; Brzezicki, M. Exploring Advancements in Bio-Based Composites for Thermal Insulation: A Systematic Review. *Sustainability* **2024**, *17*, 1143. [CrossRef]
4. Massoudinejad, M.; Amanidaz, N.; Santos, R.M.; Bakhshoodeh, R. Use of municipal, agricultural, industrial, construction and demolition waste in thermal and sound building insulation materials: A review article 09 Engineering 0912 Materials Engineering. *J. Environ. Health Sci. Eng.* **2019**, *17*, 1227–1242. [CrossRef]
5. Dilbas, H. An investigation on effect of aggregate distribution on physical and mechanical properties of recycled aggregate concrete (RAC). *J. Sustain. Constr. Mater. Technol.* **2022**, *7*, 108–118. [CrossRef]
6. Alqarni, A.S. A comprehensive review on properties of sustainable concrete using volcanic pumice powder ash as a supplementary cementitious material. *Constr. Build. Mater.* **2022**, *323*, 126533. [CrossRef]
7. Rashad, A.M. A short manual on natural pumice as a lightweight aggregate. *J. Build. Eng.* **2019**, *25*, 100802. [CrossRef]
8. Moolchandani, K. Advancements in pumice-based concrete: A comprehensive review. *Next Mater.* **2025**, *8*, 100646. [CrossRef]
9. Gómez Iborra, I.; Sanz Arauz, D. Characterization of lime based insulating mortars for existing buildings in the EU market. *MATEC Web Conf.* **2024**, *403*, 07005. [CrossRef]
10. Pokorný, J.; Pavlíková, M.; Pavlík, Z. The use of lightweight aggregate in preparation of thermal insulation lime-based renders. *Acta Polytech. CTU Proc.* **2019**, *22*, 83–87. [CrossRef]
11. Rao, P.R.; Momayez, M.; Runge, K.A.; Muralidharan, K. Recent Developments in Thermally Insulating Materials Based on Geopolymers-a Review Article. *Min. Metall. Explor.* **2020**, *37*, 995–1014. [CrossRef]
12. Gündüz, L.; Kalkan, Ş.O. Use of pumice aggregate in cementitious rheoplastic lightweight concrete. *J. Sustain. Constr. Mater. Technol.* **2023**, *8*, 57–65. [CrossRef]
13. Luo, K.; Li, J.; Lu, Z.; Wang, L.; Deng, X.; Hou, L.; Jiang, J. Preparation and performances of foamed hydraulic lime. *Constr. Build. Mater.* **2021**, *290*, 123244. [CrossRef]
14. Çoban, O.; Yilmaz, T. Volcanic particle materials in polymer composites: A review. *J. Mater. Sci.* **2022**, *57*, 16989–17020. [CrossRef]
15. Ministry of Environment, Urbanisation and Climate Change. *Notification on Expanding The Use of Green Cement with Low Carbon Emissions in Public Procurement Contracts*; Ministry of Environment, Urbanisation and Climate Change: Ankara, Türkiye, 2024.
16. Talaat Mohammed, D.; Yaltay, N. Strength and elevated temperature resistance properties of the geopolymer paste produced with ground granulated blast furnace slag and pumice powder. *Ain Shams Eng. J.* **2024**, *15*, 102483. [CrossRef]
17. De Schepper, M.; De Buysser, K.; Van Driessche, I.; De Belie, N. The regeneration of cement out of Completely Recyclable Concrete: Clinker production evaluation. *Constr. Build. Mater.* **2013**, *38*, 1001–1009. [CrossRef]
18. de Brito, J.; Saikia, N. *Recycled Aggregate in Concrete*; Springer: London, UK, 2013. [CrossRef]
19. Dilbas, H. An Investigation of the Effect of Recycled Aggregate Use on Concrete Properties. Ph.D. Thesis, Yildiz Technical University, Beşiktaş, Türkiye, 2020.

20. Çakır, Ö.; Dilbas, H. Durability properties of treated recycled aggregate concrete: Effect of optimized ball mill method. *Constr. Build. Mater.* **2021**, *268*, 121776. [CrossRef]
21. Çimsa. Çimsa EcoShine White Cement. Available online: https://cimsa.com.tr/urun/ecoshine/ (accessed on 22 September 2026).
22. Stat-Ease Inc. *Design-Expert® Software*; Stat-Ease, Inc.: Minneapolis, MN, USA, 2025. Available online: https://www.statease.com/ (accessed on 14 August 2025).
23. *TS EN 12667*; Thermal Performance of Building Materials and Products Determination of Thermal Resistance by Means of Guarded Hot Plate and Heat Flow Meter Methods Products of High and Medium Thermal Resistance. Turkish Standards Institution: Ankara, Türkiye, 2003.
24. ELEGOO. ELEGOO Neptune 4 Pro FDM 3D Printer. Available online: https://us.elegoo.com/products/elegoo-neptune-4-pro-fdm-3d-printer (accessed on 22 September 2026).
25. Leluk, K.; Frąckowiak, S.; Ludwiczak, J.; Rydzkowski, T.; Thakur, V.K. The Impact of Filler Geometry on Polylactic Acid-Based Sustainable Polymer Composites. *Molecules* **2021**, *26*, 149. [CrossRef]
26. *TS EN 771-3+A1*; Specification for Masonry Units Part 3: Aggregate Concrete Masonry Units (Dense and Lightweight Aggregates). Turkish Standards Institution: Ankara, Türkiye, 2015.
27. *TS EN 772-1+A1*; Methods of Test for Masonry Units—Part 1: Determination of Compressive Strength. Turkish Standards Institution: Ankara, Türkiye, 2015.
28. Disaster and Emergency Management Presidency. Türkiye Building Earthquake Code (TBEC 2018). In *Resmi Gazete*; Disaster and Emergency Management Presidency: Ankara, Türkiye, 2018; pp. 1–417. Available online: https://www.resmigazete.gov.tr/eskiler/2018/03/20180318M1-2-1.pdf (accessed on 29 October 2024).
29. *ASTM International C642-21*; Standard Test Method for Density, Absorption, and Voids in Hardened Concrete. ASTM International: West Conshohocken, PA, USA, 2021.
30. Jochem, L.F.; Casagrande, C.A.; Bizinotto, M.B.; Aponte, D.; Rocha, J.C. Study of the solidification/stabilization process in a mortar with lightweight aggregate or recycled aggregate. *J. Clean. Prod.* **2021**, *326*, 129415. [CrossRef]
31. Mo, K.H.; Ling, T.-C.; Alengaram, U.J.; Yap, S.P.; Yuen, C.W. Overview of supplementary cementitious materials usage in lightweight aggregate concrete. *Constr. Build. Mater.* **2017**, *139*, 403–418. [CrossRef]
32. Akpinar, E.K.; Koçyigit, F. Thermal and mechanical properties of lightweight concretes produced with pumice and tragacanth. *J. Adhes. Sci. Technol.* **2016**, *30*, 534–553. [CrossRef]
33. Velosa, A.L.; Cachim, P.B. Hydraulic-lime based concrete: Strength development using a pozzolanic addition and different curing conditions. *Constr. Build. Mater.* **2009**, *23*, 2107–2111. [CrossRef]
34. Colangelo, F.; Navarro, T.G.; Farina, I.; Petrillo, A. Comparative LCA of concrete with recycled aggregates: A circular economy mindset in Europe. *Int. J. Life Cycle Assess.* **2020**, *25*, 1790–1804. [CrossRef]
35. Kalkan, Ş.O.; Gündüz, L. The influence of anhydrite III as cement replacement material in production of lightweight masonry blocks for unreinforced non-load bearing walls. *J. Sustain. Constr. Mater. Technol.* **2022**, *7*, 322–338. [CrossRef]
36. Dilbas, H.; Birdal, F.; Parim, C.; Güneş, M.Ş. Mechanical performance improvement of super absorbent polymer-modified concrete. *MethodsX* **2023**, *10*, 102151. [CrossRef]
37. Walbrück, K.; Drewler, L.; Witzleben, S.; Stephan, D. Factors influencing thermal conductivity and compressive strength of natural fiber-reinforced geopolymer foams. *Open Ceram.* **2021**, *5*, 100065. [CrossRef]

Disclaimer/Publisher's Note: The statements, opinions and data contained in all publications are solely those of the individual author(s) and contributor(s) and not of MDPI and/or the editor(s). MDPI and/or the editor(s) disclaim responsibility for any injury to people or property resulting from any ideas, methods, instructions or products referred to in the content.